CHAPTER 4

APPROACH OF TWO FLUID PARTICLES

This chapter gives a fundamental analysis on the approach of two unequal or equal sized fluid particles and proposes two models based on the parallel film concept. A simple parallel film model giving an expression for the interaction time, disregarding all external forces, is developed based on the conservation of energy. It indicates that the interaction time is independent of the initial approach velocity and gives a good explanation why the effective virtual mass coefficient changes with the radius ratio of particles in the model of Chesters and Hofman (1982). A more general parallel film model is proposed based on the balance of forces acting on the particles. The numerical solutions of this model show how factors such as the initial velocity, the radius ratio and the buoyancy affect the interaction time, approach velocity and film area. Both models are compared to the experimental data of Scheele and Leng (1971) for the collisions of equal sized drops in the anisole-water system. The comparisons show that the general parallel film model, for the prediction of film area is in good agreement with the experimental data, but does not predict the interaction time well, possibly due to the oscillations of the drops themselves. This simple model can only be used to estimate the interaction time.

The expression of interaction time in the simple parallel film model has been used for determining the bubble coalescence efficiency in Chapter 3.

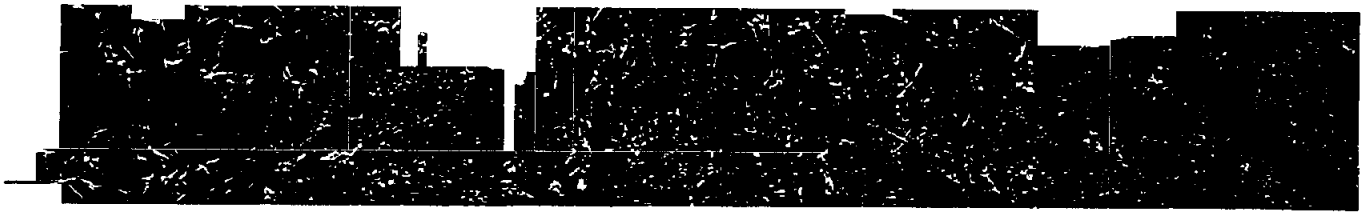

4.1 Introduction

Binary and interfacial coalescence of bubbles or drops is encountered in many industrial processes such as two and three phase separators in the petroleum industry, in extraction, absorption and distillation equipment as well as in gas-liquid or liquid-liquid reactors. It may often be a decisive factor in the design of equipment.

The coalescence of two bubbles (or drops) in liquids is usually considered to occur in three steps. First, the bubbles collide, trapping a small amount of liquid between them. This liquid then drains out until the liquid film separating the bubbles reaches a critical thickness at which film rupture occurs, resulting in coalescence. As a consequence, the coalescence process is analyzed by examining the rate of collision events and the probability of a collision resulting in coalescence. The latter depends on the time of interaction during a collision (approach) compared to the time of drainage and rupture of the film (for bubble coalescence, rupture time is usually negligible compared to drainage time). In other words, the interaction time is one of the determining factors for coalescence probability, as pointed out by Chesters (1991).

Much work has been done on determining the interaction time. However, most of it concerns the approach (or collision) processes between two equal sized particles, and the particle-interface case. For instance, Kirkpatrick and Lockett (1974) studied the bubble-bubble and bubble-interface approach and coalescence. They gave numerical solutions for the variation in the film thickness during the approach process, in absence of external forces and based on a parallel film model. Jeelani and Hartland (1991a) have proposed a model which predicts both the variation in the film area and the approach velocity during a collision and have discussed the influence of the initial approach velocity and the constant external forces acting on the particles.

Up till now, perhaps due to the complexity, very little work has been done on the interaction time for collisions between two unequal sized fluid particles, even though this case is very often encountered in practice. Therefore, in order to

determine coalescence probability, people have had to resort to assumptions. For example, a common assumption used for the approach of bubbles or drops in turbulence (Levich, 1962; Coulaloglou and Tavlarides, 1977; Lee *et al.*, 1987; Prince and Blanch, 1990), is that the interaction time is proportional to the characteristic life time of an eddy with size equal the sum of the approaching particles:

$$t_I \sim \left[(R_1 + R_2)^2 / \varepsilon \right]^{1/3} \tag{4.1}$$

In fact, this hypothesis was made by Levich (1962) mainly from dimensional analysis.

Based on the parallel film concept for equal sized particles in the case of very small Weber number, Chesters and Hofman (1982) and Chesters (1991) discussed the coalescence of two unequal sized particles, by substituting an equivalent radius in the expressions for equal sized particles, and by introducing an equivalent coefficient of virtual mass. However, even this was only for determining drainage time or coalescence time instead of interaction time.

The purpose of this work is to develop a more fundamental interaction model for the approach process valid for both two unequal and equal sized particles. The method used is based on the parallel film concept since this is the simplest, but still quite effective.

4.2 Simple Parallel-Film Model

4.2.1 Expression for film area

Consider, as shown in Figure 4.1, that an approach of two spherical bubbles (or drops) of radii R_1 and R_2 with a given initial approach velocity u_{r0} takes place under the influence of external forces including drag force. Let u_1 and u_2 denote

the velocities, relative to the mean flow of the surrounding fluid, of the centers of mass of particle *1* and *2* respectively, while v_1 and v_2 denote the relative velocities of the centers of mass of particle *1* and *2* referring to the center of mass of the two-particle system.

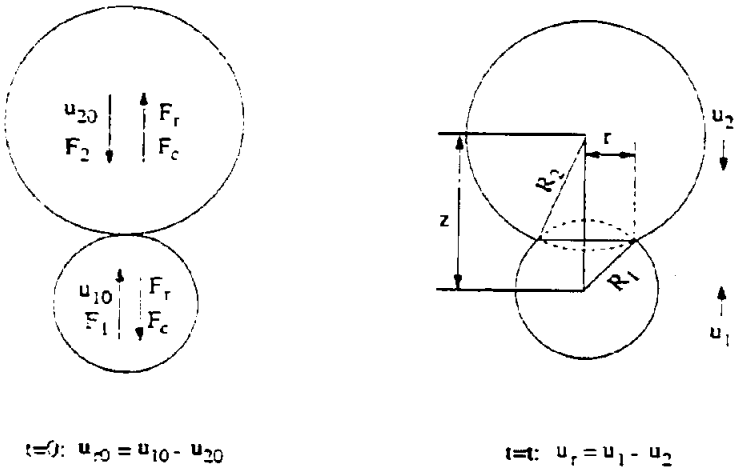

Figure 4.1 Sketch of the parallel film model

Both the two velocities, u and v, are directed along the line passing through the two particle centers of mass. At, and after the onset of flattening, they are related by the following equations,

$$u_1 = v_1 + u_{cm}, \quad u_2 = v_2 - u_{cm} \tag{4.2}$$

and

$$u_r = u_1 - u_2 = v_1 - v_2 \tag{4.3}$$

where u_r is the relative velocity between the two centers of mass of the individual particles and u_{cm} is the velocity of the center of mass of the two-particle system. The center of mass of the two-particle system moves with the velocity:

$$u_{cm} = \frac{m_1 u_1 + m_2 u_2}{m_1 + m_2} \tag{4.4}$$

The initial relative velocity can also be expressed by the individual velocities: $u_{r0} = u_{10} - u_{20}$, where u_{10} and u_{20} usually need to be known. For the approach of equal sized particles, $u_{10} = -u_{20} = u_{r0}/2$ and the system center of mass will not move ($u_{cm0} = 0$). For the approach of a particle to an interface, $u_{20} = 0$ and $m_1/m_2 \to 0$ so that $u_{cm0} = 0$, also in this case.

Assuming that the separating film thickness δ and the radius r of the deformed area are much less than the particle sizes, the increase in surface area due to the deformation can simply be expressed by

$$\Delta s = \Delta s_1 + \Delta s_2 = \frac{\pi}{4} r^4 \left(\frac{1}{R_1^2} + \frac{1}{R_2^2} \right) \tag{4.5}$$

The corresponding increase in surface free energy is $\sigma \Delta s$. For the approach of equal sized particles or a particle to an interface, it can be considered, as done by Chesters (1991), that the initial approach velocity is arrested at the last flattening stage. Assuming negligible drag, the initial kinetic energy is then fully transformed into excess surface free energy. However, for unequal sized particles, only a part of the initial kinetic energy is available for increasing the surface energy even if the effect of the drag force is disregarded. This is because the unequal particle system has a motion of the center of mass relative to the surrounding environment, *i.e.* $u_{cm} \neq 0$.

The kinetic energy of a particle system can be expressed as the sum of the internal and the translational (or orbital) kinetic energies (Alonso and Finn, 1982). For a two-particle system, this gives

$$\frac{1}{2}\left(m_1 u_1^2 + m_2 u_2^2\right) = E_{k,int} + \frac{1}{2}\left(m_1 + m_2\right) u_{cm}^2 \tag{4.6}$$

From the above equation and Equation (4.4), the internal kinetic energy can be determined by

$$E_{k,int} = \frac{1}{4} m_{eq}\left(u_1 - u_2\right)^2 = \frac{1}{4} m_{eq} u_r^2 \tag{4.7}$$

where

$$m_{eq} = \frac{2 m_1 m_2}{m_1 + m_2} \tag{4.8}$$

is the equivalent mass of the two-particle system. In the above equation m_i (i = 1 or 2) is the actual plus the virtual mass of a particle:

$$m_i = \frac{4\pi}{3} \rho_c R_i^3 \left(\frac{\rho_d}{\rho_c} + \gamma \right) \tag{4.9}$$

Here γ is the coefficient of virtual mass normally taken to be a constant between 0.5 and 0.8 (Jeelani and Hartland, 1991a). A value of 0.5 has been deduced theoretically for spherical rigid particles in potential flow (Maxey and Riley, 1983) and 0.25 was used by Cook and Harlow (1986) for deformed bubbles in water. Geary and Rice (1991) and Jeelani and Hartland (1991a) suggested 0.69 for spherical bubbles and Chesters (1991) has used 0.75 for the same case.

Combining Equations (4.8) and (4.9) the equivalent mass of a two-particle system can be expressed by

$$m_{eq} = \frac{2 m_1}{1 + \xi^3} = \frac{8\pi}{3} \rho_c R_1^3 \frac{\rho_d / \rho_c + \gamma}{1 + \xi^3} \tag{4.10}$$

where the particle radius ratio, $\xi = R_1/R_2$.

Now, considering that the increase in surface energy at the final flattening stage, when the maximum film area is obtained, stems from the loss of initial internal kinetic energy, $\sigma\Delta s = E_{k,int}$, this gives

$$\frac{\pi}{4} r_{max}^4 \left(R_1^{-2} + R_2^{-2}\right)\sigma = \frac{1}{4} m_{eq} u_{r0}^2 \tag{4.11}$$

It can be seen that this energy balance relationship reduces to that for two equal sized particles developed by Chesters (1991), as $R_1 = R_2$, $m_1 = m_2$ and $u_{10} = -u_{20} = u_{r0}/2$, and to that for a particle moving towards an interface as $R_2 \rightarrow \infty$, $m_2 \rightarrow \infty$ and $u_{10} = u_{r0}$ ($u_{20} = 0$).

Denoting $A = (r/R_1)^2$ and $u_r^* = u_r(\rho_c R_1/\sigma)^{1/2}$, the energy balance relationship, Equation (4.11), is rewritten as

$$A_{max}^2 = \frac{m_{eq} u_{r0}^2}{\pi\left(R_1^{-2} + R_2^{-2}\right) R_1^4 \sigma} = \lambda We \tag{4.12}$$

where

$$\lambda = \frac{8\left(\rho_d/\rho_c + \gamma\right)}{3\left(1+\xi^2\right)\left(1+\xi^3\right)} \tag{4.13}$$

and

$$We = \frac{R_1 \rho_c u_{r0}^2}{\sigma} = u_{r0}^{*2} \tag{4.14}$$

Since the value of λ is approximately between 1/3 and 4/3, the requirement, $r_{max} < R_1$, corresponds to the condition of the Weber number being very small.

4.2.2 Expression for interaction time

Denoting z as the distance between the centers of the two bubbles, as shown in Figure 4.1, then

$$z = R_1 + R_2 - \frac{1}{2}R_1(1+\xi)(r/R_1)^2 = R_1 + R_2 - \frac{1}{2}R_1(1+\xi)A \qquad (4.15)$$

Assuming, analogous to Chesters (1991), that the centers of mass of the two particles are the same as their geometrical centers, then $R_1+R_2-z_{max}$ indicates the distance that the two particles have moved when the film area reaches its maximum. The time needed for this approach process, t_{max}, which was defined as the interaction time by Chesters (1991), is found to approximately equal $(R_1+R_2-z_{max})/u_{r0}$. Here z_{max} can be determined by Equations (4.12) and (4.15) setting $z = z_{max}$ and $A = A_{max}$. Hence, the interaction time can be expressed in dimensionless form as

$$\tau_{max} = \frac{1}{2}(1+\xi)\sqrt{\lambda} \qquad (4.16)$$

where the dimensionless time, τ, is defined by

$$\tau = t\left(\frac{\sigma}{\rho_c R_1^3}\right)^{1/2} \qquad (4.17)$$

In Equation (4.16) it is assumed that the time for the film area to go from zero to its maximum equals the time for the reverse process back to zero and indi-

cates that the interaction time not only depends on the properties of the fluids used, but also on the radius ratio of the two approaching particles. It also shows that the interaction time is the same for $\xi = 1$ (two equal sized particles) and $\xi = 0$ (a particle to an interface). However, the dimensionless interaction time is independent of the initial approach velocity.

Often, for both equal and unequal sized particles, the centers of mass of the two particles are different from their geometrical centers due to particle deformation. When this variation is considered, it can be shown that the approach distance that the two particles have moved is better expressed by

$$R_1 + R_2 - z_{max} = \frac{3}{16}(1+\xi^3)R_1 A_{max}^2 \tag{4.18}$$

Taking this into account, the dimensionless interaction time becomes

$$\tau_{max} = \frac{1}{2}\left[1 - \frac{3}{8}(1-\xi+\xi^2)\sqrt{\lambda We}\right](1+\xi)\sqrt{\lambda} \tag{4.19}$$

This result shows that since the Weber number in this simple parallel film model should be very small, the influence of the variation of the centers of mass due to particle deformation on the interaction time may be ignored.

4.2.3 Virtual mass coefficient

As discussed above, for two unequal sized particles, not all the initial kinetic energy is transformed to increase the surface energy. In order to describe the case of unequal sized particles (for discussing the film drainage), Chesters and Hofman (1982) and Chesters (1993) introduced an effective coefficient of virtual mass, γ_{eff} to describe the available kinetic energy, $E_{k,avl}$, leading to the increase in surface energy:

$$E_{k,avl} = \gamma_{eff} \frac{\pi}{4} \rho_c R_{eq}^3 u_{r0}^2 \tag{4.20}$$

where

$$R_{eq} = \frac{2R_1 R_2}{R_1 + R_2} = \frac{2R_1}{1+\xi} \tag{4.21}$$

is the equivalent radius defined by Chesters and Hofman (1982). The authors found that the effective coefficient of virtual mass changed with the particle radius ratio and also gave some values for various radius ratios using an indirect method. The values given were about 1 for $\xi = 1$ and about 1/4 for $\xi \to 0$.

In fact, since the available kinetic energy is only the internal part, or $E_{k,avl} = E_{k,int}$, the effective coefficient of virtual mass can be expressed as

$$\gamma_{eff} = \frac{(1+\xi)^2(\rho_d/\rho_c + \gamma)}{3(1-\xi+\xi^2)} \tag{4.22}$$

Taking $\gamma = 0.69$, for bubbles, the values of the effective coefficients calculated by the above relationship are 0.92 and 0.23 for $\xi = 1$ and $\xi \to 0$ respectively, and if taking $\gamma = 0.75$, the results are 1.0 and 1/4. The latter results correspond to those obtained by Chesters and Hofman (1982). Therefore, this model gives a theoretical explanation why the effective coefficient of virtual mass introduced by Chesters and Hofman (1982) is a function of the particle radius ratio. That is, there is a fraction of the initial kinetic energy that does not convert into the excess surface energy for two unequal sized particles. This fraction is dependent on the radius ratio.

4.3 General Parallel-Film Model

Because the assumption, $r_{max} < R_1$ ($R_1 \leq R_2$), has been employed in the simplified parallel film model developed above, the expressions of interaction time and film area are, as mentioned, only suitable for cases with very small Weber numbers. This can not be satisfied for many practical processes and it is therefore necessary to develop a more general model without this assumption.

According to Figure 4.1, a general force balance in the direction along the line passing through the particle centers of gravity gives

$$m\frac{du}{dt} = F - F_c - F_r \tag{4.23}$$

The drag force can be expressed as $F_r = 12\pi\mu_c R u$ and the restoring force (capillary force) as $F_c = \beta\sigma\pi r^2/R$. Here β is a parameter determining the excess pressure in the film (Jeelani and Hartland, 1991a) and depends on the real radii of curvature of the film and thereby changes with time (Chesters and Hofman, 1982). In the parallel film model, for simplification, it is usually assumed to be constant. For a plane film $\beta = 2$ but for a convex film β is less than 2. A value $\beta = 1$ was used by Jeelani and Hartland (1991a) for a deformed interface when a particle approaches an interface. However, the parameter may be larger than 2 for a concave film.

By inserting the force terms for the individual bubbles, the above equation can be written as

$$m_1\frac{du_1}{dt} = F_1 - \frac{\beta_1\pi\sigma r^2}{R_1} - 12\pi\mu_c R_1 u_1 \tag{4.24}$$

and

$$m_2 \frac{du_2}{dt} = F_2 - \frac{\beta_2 \pi \sigma r^2}{R_2} - 12\pi\mu_c R_2 u_2 \tag{4.25}$$

Subtracting Equation (4.25) from Equation (4.24), an equation describing the approach motion between two unequal sized particles, after the onset of flattening, is obtained:

$$\frac{du_r}{dt} = \frac{F_1 - \xi^3 F_2}{m_1} - \frac{\pi\sigma r^2(\beta_1 + \beta_2\xi^2)}{m_1 R_1} - \frac{12\pi\mu_c R_1(u_1 - \xi^2 u_2)}{m_1} \tag{4.26}$$

The change of the radius ratio, ξ, with time has been ignored and the relationship, $m_1/m_2 = \xi^3$, has been used in the above equation. In reality, the particle shapes vary with time due to the deformation during an approach and then the radius ratio may change with time for unequal sized particles (For equal sized particles, no matter the degree of flattening of the individual particles, the radius ratio keeps constant at unity ($\xi \equiv 1$) because the deformation is identical for both particles). For unequal sized particles, the radius change of the smaller particle is greater than that of the larger one, and thereby the smaller the initial radius ratio, the greater the change of radius ratio with time. However, the change is usually insignificant when $A < 1$. For example, even if $\xi = 0$ and $A = 0.9$, the radius ratio variation from its initial value is only about 11%. Therefore the omission of the change in radius ratio in Equation (4.26) seems acceptable.

The parameters, $\beta_1 = \beta_2 = 2$, for a plane film, but $\beta_1 \neq \beta_2$ for a deformable film. If β_1 is less than 2 (convex film for bubble *1*) then β_2 will be larger than 2 (concave for bubble 2).

Combining Equations (4.4) and (4.2) with Equation (4.3) gives

$$v_1 = \frac{u_r}{1 - \xi^3}, \qquad v_2 = -\frac{u_r \xi^3}{1 + \xi^3} \tag{4.27}$$

Therefore, Equation (4.26) may be rewritten in dimensionless form as

$$\frac{du_r^*}{d\tau} = -\lambda_1 A - \lambda_2 S_f u_r^* - \lambda_3 S_f u_{cm}^* + F_I^* \tag{4.28}$$

where

$$\lambda_1 = 0.75\frac{\beta_1 - \beta_2\xi^4}{\rho_d/\rho_c + \gamma} \tag{4.29}$$

$$\lambda_2 = \frac{9(1+\xi^5)}{(\rho_d/\rho_c + \gamma)(1+\xi^3)} \tag{4.30}$$

$$\lambda_3 = \frac{9(1-\xi^2)}{\rho_d/\rho_c + \gamma} \tag{4.31}$$

$$F_I^* = \frac{0.75(F_1 - \xi^3 F_2)}{\pi R_1 \sigma(\rho_d/\rho_c + \gamma)} \tag{4.32}$$

and the surface force number (a kind of capillary number) is defined by

$$S_f = \mu_c(\rho_c R_1 \sigma)^{-1/2} \tag{4.33}$$

Equation (4.28) is the general approach equation of two equal or unequal particles based on the parallel film model. However, this equation is only valid for values of A less than unity since the change of the radius ratio is disregarded.

Denoting z as the distance between the centers of mass of the two particles, the instantaneous relative velocity can then simply be determined by $u_r = -dz/dt$. The

negative sign is set so that the velocity is positive when the two particles move close. When the deformation of the smaller particle or the value of A is not too large, it is possible to assume that the centers of mass of the individual particles do not change with time during the flattening process, and remain the same as their geometrical centers. However, for larger value of A, the variations of the centers of mass from the corresponding geometrical centers are significant and the center of mass for both particles usually shifts to their rear. Thus, the distance between the centers of mass of the two particles, z, can be expressed by two parts: the distance between their geometrical centers and the shifts of the centers of mass from their geometrical centers:

$$\frac{z}{R_1} = (1-A)^{1/2} - \frac{(1-\xi^2 A)^{1/2}}{\xi} + \frac{3}{16}(1-\xi^3)A^2 \tag{4.34}$$

where the first two terms on the right hand constitute the distance between the geometrical centers of the particles.

Therefore, the instantaneous velocity can be written as

$$u_r^* = \frac{1}{2}\left[\frac{1}{(1-A)^{1/2}} - \frac{\xi}{(1-\xi^2 A)^{1/2}} - 0.75(1-\xi^3)A\right]\frac{dA}{d\tau} \tag{4.35}$$

The center of mass of a system of particles moves as if it were a particle of mass equal to the total mass of the system and subject to the external forces applied to the system (Alonso and Finn, 1982). Hence for a two-particle system, the equation of motion is

$$(m_1 + m_2)\frac{du_{cm}}{dt} = (F_1 - F_2) - 12\pi\mu_c(R_1 - R_2)u_{cm} \tag{4.36}$$

Its dimensionless form is

$$\frac{du_{cm}^*}{d\tau} = F_{II}^* - \lambda_4 s_f u_{cm}^* \tag{4.37}$$

where

$$\lambda_4 = \frac{9\xi^2}{(\rho_d/\rho_c + \gamma)(1 - \xi + \xi^2)} \tag{4.38}$$

and

$$F_{II}^* = \frac{0.75(F_1 + F_2)\xi^3}{\pi R_1 \sigma (1 + \xi^3)(\rho_d/\rho_c + \gamma)} \tag{4.39}$$

When the change in radius ratio is negligible, an analytical solution for Equation (4.37) can be obtained

$$u_{cm}^* = \frac{F_{II}^*}{\lambda_4 S_f} + \left[u_{cm0}^* - \frac{F_{II}^*}{\lambda_4 S_f} \right] \exp(-\lambda_4 S_f \tau) \tag{4.40}$$

Equations (4.28) and (4.35) are a set of two first order ordinary differential equations and can be expressed as one second order ordinary differential equation, which can easily be solved by using Runge-Kutta methods. Some of the numerical results will be discussed in the following section.

These equations reduce to the equation for the approach of two equal sized particles or a bubble to an interface developed by Jeelani and Hartland (1991a) when $\xi = 1$ (here $F_2 = -F_1$) or $\xi = 0$ (here $F_2 = 0$). In addition, for these cases, analytical solutions for the dimensionless velocity and film area can be obtained by assuming that $r \ll R_1$ and that the drag force is negligible, as done by Jeelani and Hartland (1991a).

4.4 Results and Discussion

4.4.1 Zero external force

The first case discussed here is when external forces are absent or negligible. The variations of the film area and the approach velocity with time then depend only on the initial approach velocity and the radius ratio for a given system.

For the case of equal sized bubbles of air in water, Figure 4.2 and Figure 4.3 show how the values of the dimensionless approach velocity, u_r^*, and the dimensionless film area, A, change with the dimensionless time, τ, at various initial approach velocities u_{r0}^*. u_r^* decreases from its initial value to zero and then becomes negative when the bubbles rebound until the negative maximum is reached. On the other hand, the corresponding value of A increases from zero up to a maximum value A_{max} when u_r^* equals zero (the kinetic energy of the relative motion between the two bubbles is zero) and then decreases to zero when u_r^* becomes a negative extreme, because the bubbles rebound and the excess surface energy is transformed back into kinetic energy.

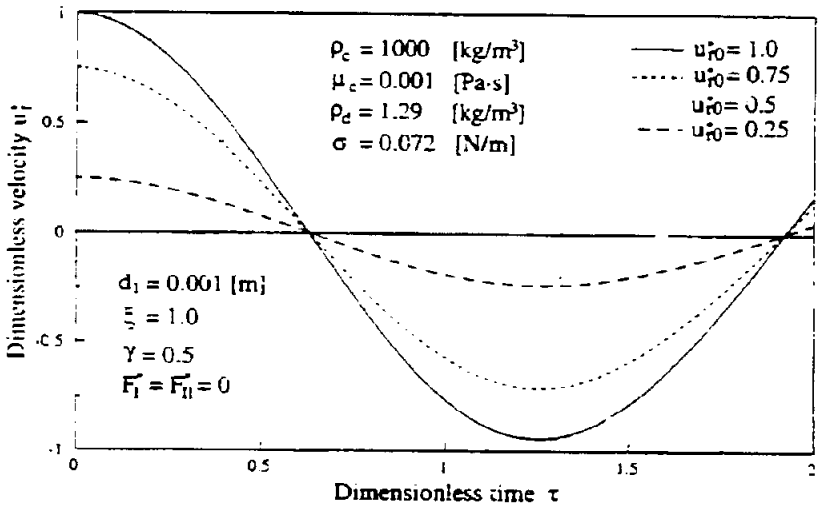

Figure 4.2 Variation of u_r^* with τ

However, when the value of A returns to zero the absolute value of u_r^* is not restored to its original initial value, since some of the initial kinetic energy has been consumed by the viscous resistance against the relative motion between the two bubbles (there is no relative motion between the center of mass of the two-bubble system and the surrounding liquid since we here consider the case of two equal sized bubbles).

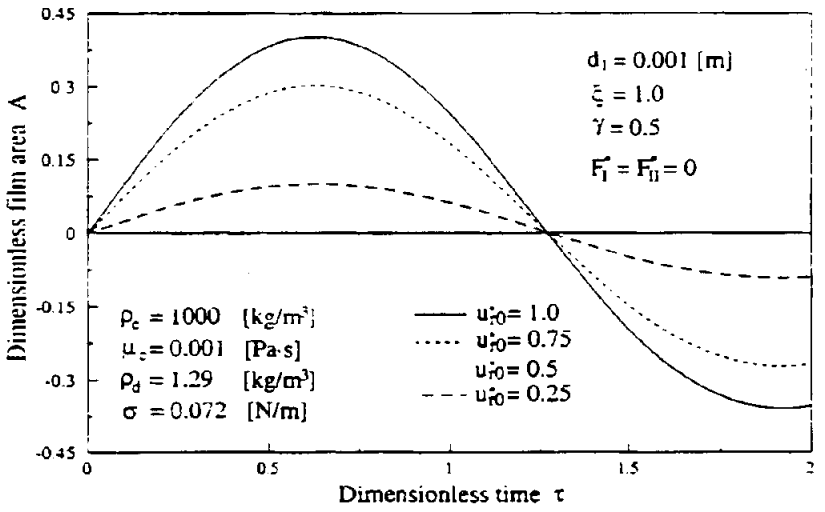

Figure 4.3 Variation of A with τ

The value of A_{max} obtainable increases with increasing initial approach velocity, u_{r0}^*. This is reasonable since larger values of u_{r0}^* supply higher initial kinetic energy. In addition, the dimensionless time needed for the film area to reach A_{max} from zero, τ_{max}, is independent of the initial approach velocity. This time is the same as the definition of interaction time in the simple parallel film model expressed by Equation (4.16). Equation (4.16) also shows that τ_{max} only relies on the radius ratio and the coefficient of virtual mass and is independent of the particle size, R_1, in the absence of external forces. When A_{max} is not too large (< 0.5), the interaction times estimated by Equation (4.16) are usually less than, but close to those found by the numerical solution of the general parallel film

model, *e.g.* the values of τ_{max} for the air-water system are approximately 0.58 and 0.62 estimated by the former and the latter respectively, when $\gamma = 0.5$ and $\xi = 1$ or 0. This discrepancy is reasonable since the interaction time estimated by the simple parallel film model assumes a constant approach velocity with the same value as the initial one instead of a variable approach velocity decreasing with time as in the general parallel film model.

The results show that the effect of viscous drag may not be negligible even for low viscosity systems as air-water, especially for small fluid particle sizes. The effects of liquid viscosity and surface tension on both u_r^* and A are presented in Figure 4.4 and Figure 4.5. An increase of viscosity and a decrease in surface tension make u_r^* and A decrease. The effect on τ_{max} is a small reduction. This effect of surface tension on τ_{max} can also be found in the simple parallel film model through the Weber number in Equation (4.19). According to Figure 4.4 and Figure 4.5, viscosity has a more significant effect than surface tension.

The effect of the bubble radius ratio on u_r^* and A at a given size of bubble 1 (d_1 = 0.001 m) is shown in Figure 4.6 and Figure 4.7. Reducing the radius ratio, ξ, leads to a slower decrease in u_r^* and an increase τ_{max}. After reaching a radius ratio of 0.5, u_r^* decreases quicker with time again. At radius ratios above 0.5 the initial approach velocity is contributed to by the two bubbles and the smaller bubble moves with the larger one, relative to their surrounding liquid. The approach velocity will thereby decrease more slowly with decreasing ξ. When the radius ratio is very small the initial approach velocity is determined by the smaller bubble since it has a mass much smaller than the larger one (at $\xi = 0$ the velocity of the larger bubble is zero — the case of a bubble approaching an interface) and then the approach velocity decreases faster again, thus reducing τ_{max}. In the absence of external forces, when $\xi \to 0$ the curve for the velocity is the same as that for $\xi = 1$.

The maximum value of A, however, always increases with decreasing radius ratio. This is understandable, because in reaching the same film area (the same excess surface energy), the smaller the radius ratio, the more the bubble with radius R_1 "invades" into the larger bubble, as shown in Figure 4.1.

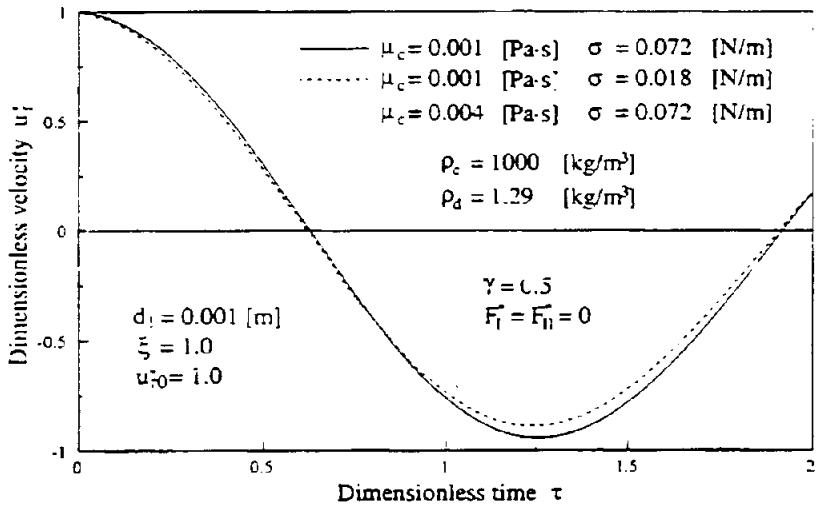

Figure 4.4 Variation of u_r^* with τ

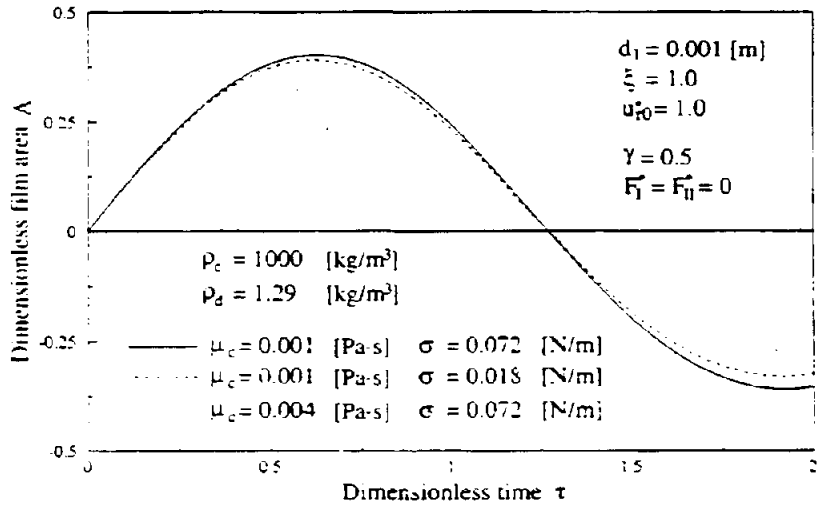

Figure 4.5 Variation of A with τ

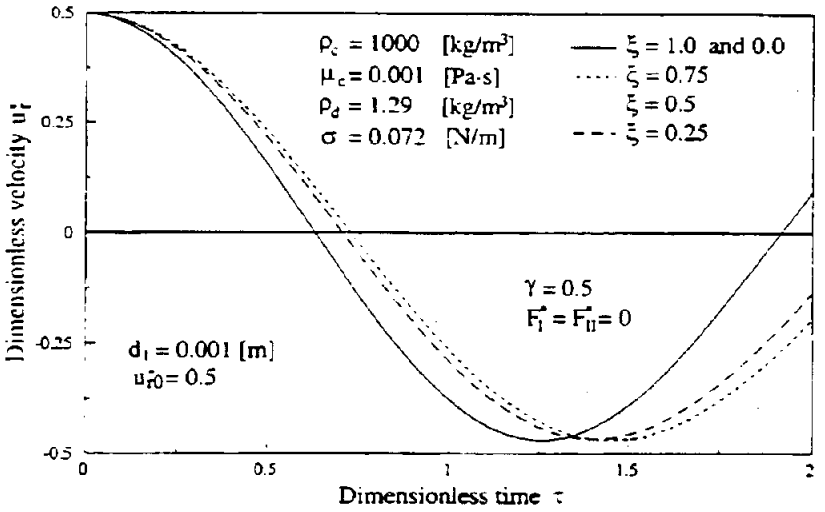

Figure 4.6 Variation of u_r^* with τ

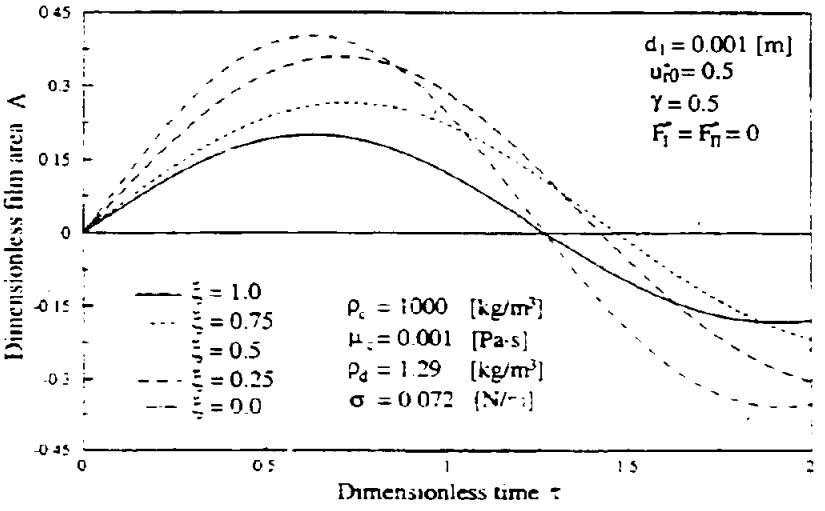

Figure 4.7 Variation of A with τ

If one assumes an initial approach velocity independent of bubble size, the bubble size itself has nearly no effect on A, u_r^* and τ_{max} for a given initial approach velocity, according to the numerical results of the general parallel film model (not shown by figures). However, in fact, the initial approach velocity and external forces are almost always dependent upon the particle sizes. Thus the effect of particle sizes is reflected by the initial approach velocity and/or the external forces.

The simple parallel film model also shows only a small effect of particle sizes on τ_{max}, as expressed by Equation (4.16) or (4.19). However, this does not mean that the particle size has a small effect on the interaction time since $t_{max} = \tau_{max}(\rho_c R_1^3/\sigma)^{1/2}$.

The periodic property of the curves of A and u_r^* with time is a mathematical consequence of the parallel film model used.

4.4.2 Effect of external forces

For many cases in practice, the effect of external forces acting on the approaching particles is not negligible, *e.g.* in the approach of a bubble to an interface the buoyancy force clearly exists. In addition, the external forces acting on the particles are usually connected to the particle sizes, *e.g.*, the buoyancy for particle 1 is $(\pi/6)d_1^3\Delta\rho g$. Figure 4.8 and Figure 4.9 show the effect of external forces in the air-water system for the case of equal sized particles where $F_1 = -F_2$, and with values of forces independent of particle size. The dimensionless force, F_1^*, indicates the ratio of external forces to surface forces. An increase in F_1^* always makes u_r^*, A and τ_{max} increase. When $F_1^* < 0.1$, the effect of the external forces is negligible. When the external forces are of the same order as, or larger than the surface forces ($F_1^* \approx 1$ or > 1), u_r^* will increase with time, for a short period at the beginning of the bubble approach.

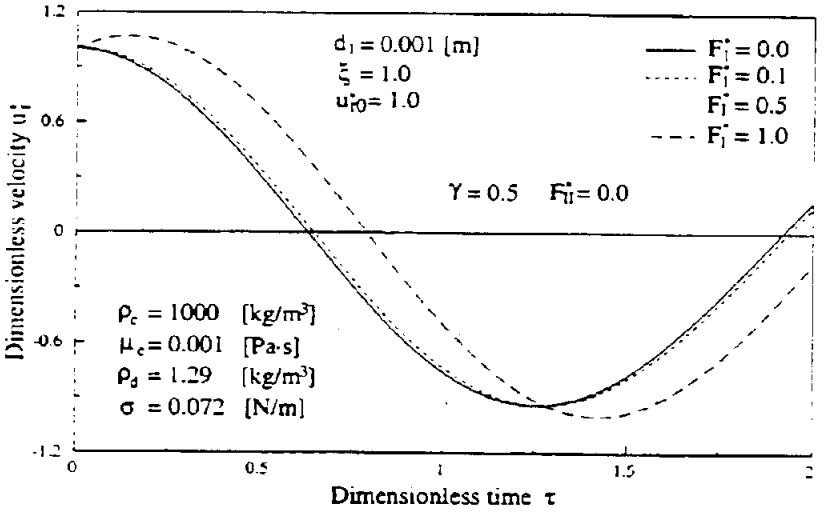

Figure 4.8 Variation of u_r^* with τ

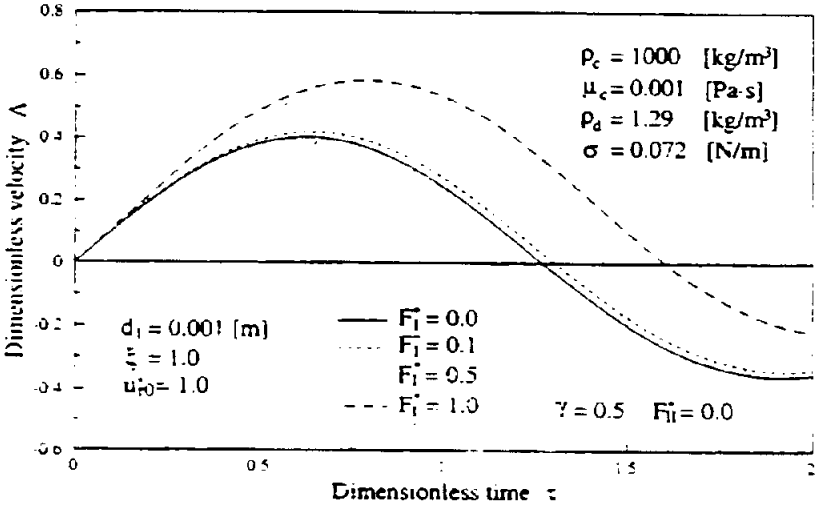

Figure 4.9 Variation of A with τ

In the general parallel film model, both the initial approach velocity and the external forces are important for the film area and the interaction time if their magnitudes are of the same order. Only when $F_f^* \gg u_{r0}^*$ may the effect of the initial approach velocity be negligible. This contradicts the conclusion of Jeelani and Hartland (1991a) who stated that the initial approach velocity could be disregarded compared to the buoyancy in the case of a bubble approaching an interface. For example, for a bubble with diameter 0.001 m moving towards an interface in the air-water system, $F_f^* = 0.0681$ and $u_{r0}^* = 0.316$ so that the external forces could be disregarded instead of the initial approach velocity.

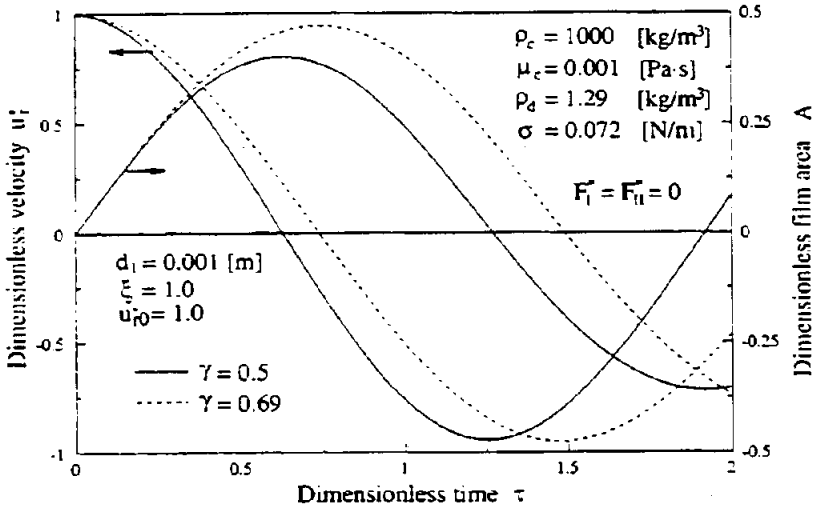

Figure 4.10 Variation of u_r^* and A with τ

4.4.3 Effect of virtual mass

Figure 4.10 shows the effect of the coefficient of virtual mass, γ, for the air-water system with $\xi = 1$ in the absence of external forces. The effect is very significant in this gas-liquid system. An increase in γ will make the effective mass of the particles larger, making u_r^* decay slower due to large inertia, and increasing the maximum value of A obtainable due to increased initial kinetic

energy. The effect of γ is expected to be less significant in a liquid-liquid system since the effective mass is proportional to $\rho_d/\rho_c+\gamma$, where the relative increase of the effective mass is about 13%. In the air-water system it is about 40% when γ shifts from 0.5 to 0.69.

In our models, the density of the dispersed phase, ρ_d is always combined with the coefficient of virtual mass, γ, so that its effect is similar to that of the coefficient of virtual mass. However, for gas-liquid systems at low pressure, the effect of changes in the gas density can be disregarded.

4.4.4 Comparison with experimental data

Unfortunately no approach data for two unequal sized particles have been found in the literature. Approach data for equal sized anisole drops in water have been reported by Scheele and Leng (1971), and are compared to the parallel film model results as shown in Table 4.1. The authors recorded the collision processes by using a high speed camera and reported 23 runs of collisions resulting in 7 cases of coalescence and 16 rebounds. Only the 16 rebound data are used for comparison because only for these are the values of A_{max} and τ_{max} available. The drop diameters for all the runs were 0.0034 ± 0.00015 m and the physical properties used in the calculations were given by the authors: ρ_c = 997.5 kg/m^3, ρ_d = 988.6 kg/m^3, $\mu_c = 8.94\times10^{-4}$ Pa·s and σ = 0.0255 N/m. The coefficient of virtual mass used for modeling was 0.5.

From Table 4.1, it can be seen that the predictions for A_{max} are quite good when using the general parallel film model (GPFM). If tuning the drop sizes in the range of 0.0034 ± 0.00015 m even better fits for A_{max} can be obtained. The predictions for τ_{max} are not so good and the errors seem to occur randomly. However, an explanation for the discrepancies in the predictions of τ_{max} may be sought in the effect of the drop oscillation phase angle, θ, at the moment of contact between the drops. Very clear oscillations of the drop size in the direction of motion were reported by Scheele and Leng (1971), while the models in this work do not include this phenomenon. However, the effect may be consid-

ered by introducing an additional oscillation force or velocity, as done by Jeelani and Hartland (1991b). They have shown that an additional oscillation force with five tuning parameters, which were different for the various runs, could well fit the data of Scheele and Leng (1971).

Table 4.1 Comparison with the experimental data of Scheele and Leng (1971)

	Data measured by Scheele and Leng (1971)				GPFM		SPFM	
Run	θ	u^*_{r0}	A_{max}	τ_{max}	A_{max}	τ_{max}	A_{max}	τ_{max}
2	260	0.386	0.299	1.147	0.272	1.09	0.385	0.997
3	207	0.438	0.299	0.887	0.309	1.09	0.437	0.997
4	210	0.436	0.312	0.693	0.308	1.09	0.435	0.997
5	217	0.475	0.299	0.707	0.334	1.09	0.473	0.997
6	230	0.445	0.360	0.599	0.314	1.09	0.444	0.997
7	180	0.361	0.256	1.248	0.254	1.09	0.359	0.997
8	150	0.394	0.274	1.465	0.278	1.09	0.393	0.997
9	165	0.396	0.280	1.364	0.279	1.09	0.394	0.997
10	180	0.378	0.374	1.291	0.266	1.09	0.377	0.997
12	285	0.261	0.221	2.799	0.183	1.09	0.260	0.997
13	330	0.242	0.233	2.547	0.170	1.09	0.242	0.997
14	345	0.868	0.585	2.244	0.598	1.09	0.865	0.997
20	345	0.774	0.621	2.576	0.539	1.09	0.772	0.997
22	315	0.568	0.426	2.460	0.400	1.09	0.566	0.997
23	240	0.262	0.256	2.063	0.184	1.09	0.261	0.997
24	330	0.157	0.109	1.898	0.110	1.09	0.157	0.997

In the measurements of Scheele and Leng (1971), the pairs of drops were simultaneously launched from two opposing nozzles controlled by magnetic variable pulse generators. This may be the reason why such strong oscillations appeared. The phase angle at contact of two drops was found to be a very significant parameter in determining the occurrence of coalescence, *e.g.* for all 7 cases of coalescence θ was between 0° and 127°. For the 16 rebounds, θ was between 150° and 345°. For phase angles of 0-180° the drop front surfaces will retreat as a result of the oscillation during the approach process. This may result in a lower effective approach velocity for the drop front surfaces and a slower increase in film area (Scheele and Leng, 1971) and thereby a longer interaction time with an increased chance for coalescence. However, the oscillations of the

drop surfaces have little effect on the initial kinetic energy in an approach process and are not important for determining A_{max}.

Figure 4.11 shows the phase angle at contact for the drop pairs of Scheele and Leng (1971). From this figure, some indications concerning the discrepancies between the experimental interaction times and the predictions can be obtained:

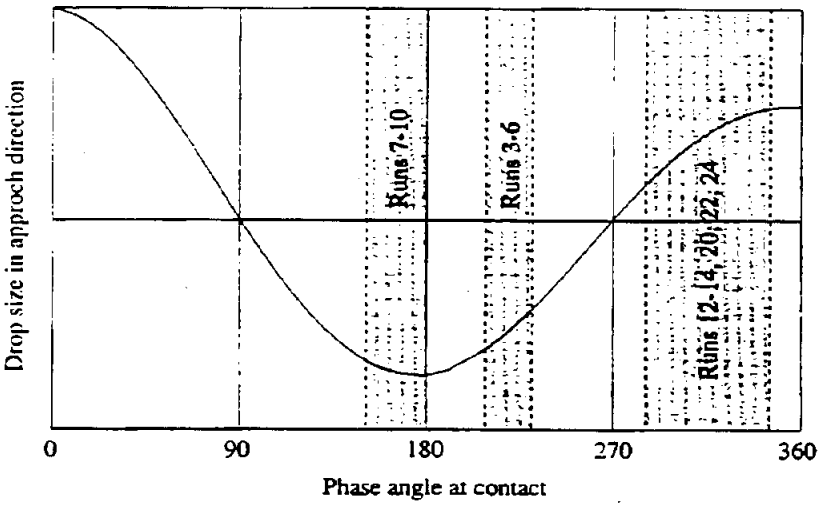

Figure 4.11 The sketch of oscillation of drops versus phase angle.

(1) For runs 3-6 it is not unreasonable that the measured values of τ_{max} (about 0.6-0.9) are on the lower side compared to the predicted value of 1.09. Their phase angles are in the range of 207-230° meaning that they are in a process of size expansion in the approach direction. This equivalently increases the approach velocity between the drop front surfaces and thereby makes the film area increase faster. Thereby the film area can reach its maximum earlier than without oscillations. For the collision of run 3, as an example, θ = 207°, and the size expansion in the approach direction will continue for a time interval, Δt = 0.05*(360-207)/360 = 0.0213 s (under the experimental conditions, 360° = 0.05 s) or $\Delta\tau$ = 1.54. Hence, within the time interval of t_{max} = 0.0123 s (τ_{max} = 0.887) the drop front surfaces will always be expanding and this results in a faster

increase in film area.

(2) For runs 12-14, 20, 22 and 24 that have phase angles in the range of 285-345°, the drop front surfaces first tend to expand, which increases the approach velocity between the front surfaces. However, after $\Delta\tau = 0.15$-0.75, which is only 8-27% of the corresponding values of τ_{max} (about 1.9-2.8), the front surface expansion shifts to retreat for the remaining part of the approach, until a maximum film area is reached, thereby giving experimental values of τ_{max} higher than the predictions, which do not consider the oscillations.

(3) For runs 7-10 that have phase angles between 150-180° at the moment of contact, the drop front surfaces first tend to retreat, which lowers the approach velocity for the front surfaces and thereby retards the increase in film area. However, since the phase angles for the runs are close to 180°, the drop front surfaces first retreat slowly, but soon shift to expansion (within $\Delta t \approx 0.0042$ s or $\Delta\tau \approx 0.3$). This reduces the chances for coalescence and may be the reason why the total discrepancies between experimental and predicted results are acceptable for the runs, and also explain the slight high values obtained (τ_{max} about 1.2-1.5 compared to 1.09).

If one uses $\gamma = 0.69$ instead of 0.5, then τ_{max} will increase from 1.09 to 1.16 and A_{max} will be about 6% higher as those when $\gamma = 0.5$. This shows that the effect of γ is fairly insignificant for this liquid-liquid system.

Clearly, the predicted values of A_{max} by Equation (4.12) of the simple parallel film model (SPFM) for all cases are too large. This is thought mainly due to the model requirement, $r_{max} \ll 1$. However, the discrepancy in prediction of τ_{max} between the GPFM and the SPFM is not very large. This may be the result of, at the same time using u_{r0} as the approach velocity for the whole approach process instead of a decreasing approach velocity, while

$$t_{max} = (1+\xi)\frac{R_1 A_{max}}{2u_{r0}} \tag{4.41}$$

for this model. Hence, the simple parallel film model may be used to estimate the interaction time when an algebraic expression for the time is desired.

4.5 Conclusion

The models developed tempt to give more a fundamental analysis of the approach process of two unequal or equal sized particles by using the parallel film concept. The influence of the special characteristics of the unequal sized particle system, such as the motion of the center of mass and the variation of the center of mass of a particle from its geometrical center, has been considered.

A simple algebraic expression for the interaction time, τ_{max}, excluding the influence of external forces has been developed based on the conservation of energy. The simple expression indicates that the interaction time is independent of the initial approach velocity in absence of external forces, which is in agreement with the numerical solution of the general parallel film model proposed. It also gives a good explanation why the effective coefficient of virtual mass changes with the radius ratio of particles in the model of Chesters and Hofman (1982).

A general parallel film model for the approach between two unequal or equal sized particles is proposed based on the balance of the forces acting on the particles during the approach process. The numerical solutions of this model show how variables such as the initial velocity, the radius ratio of particles and the buoyancy affect the interaction time, approach velocity and the maximum film area.

Both models have been compared with the experimental data of Scheele and Leng (1971) for collisions between equal sized drops in the anisole-water system. The comparison shows that the general parallel film model predictions for the maximum film area, A, agree well with the experimental data but that significant deviations occur for the interaction time, τ_{max}. The discrepancies can

in part be explained by the shape oscillations of the drops in the approach direction. However, it is possible to consider the oscillation effect by introducing an additional oscillation force, or velocity, into the general parallel film model (Jeelani and Hartland, 1991b).

The prediction results for the interaction time, τ_{max}, by the simple parallel film model of Equation (4.12) are close to those obtained by the general parallel film model. Hence, this equation can be used as an estimate of the interaction time.